An Advanced Euler-Lagrange Approach to Numerical Simulation of Cavitating Engeneering Flows

Sergey Yakubov Bahaddin Cankurt Patrick Schiller

Moustafa Abdel-Maksoud Thomas Rung

Institute of Fluid Dynamics and Ship Theory (M-8)
University of Technology Hamburg-Harburg
Schwarzenbergstraße 95C, 21073 Hamburg, Germany
E-Mail: sergey.yakubov@tu-harburg.de, Web page: http://www.tu-harburg.de/fds

SUMMARY

State-of-the-art approaches to cavitation modelling, their drawbacks and benefits are discussed in the paper. A combination of the Euler-Euler and Euler-Lagrange approaches aimed to reduce computational time is suggested. Numerical results for a challenging industrial application, such as cavitating five-blade controllable pitch propeller flow are presented and compared with the experiments. The proposed method allows to perform accurate cavitation predictions in a reasonable amount of wall-clock time.

INTRODUCTION

An Euler-Lagrange approach to two-phase liquid-vapor flow modelling has been recently suggested as an alternative to a widely used volume-of-fluid (VoF) based Euler-Euler methods [2, 13]. In this approach vapor is considered as a discrete phase, composed of individual bubbles. Bubble dynamics in surrounding liquid is governed by Newtonian equations of motion coupled with the Rayleigh-Plesset equation for the description of the vaporisation/condensation process. With such an approach various forces acting on an individual bubble as well as water quality effects can be taken into account providing more accurate prediction of cavitation patterns [6]. However, it should be mentioned that Euler-Lagrange approaches require significant computational resources due to the large number of tracked bubbles and micro time scales. Therefore, advanced high performance strategies are needed [16].

Reliable prediction of cavitating flows is of a high importance in marine applications, turbomachinery, chemical and biomedical applications. Recently performed joint simulation exercises for a cavitating propeller displayed that Euler-Euler cavitation models in general give a fair agreement with the experiments for the global engineering parameters [1]. Nevertheless, it was shown that results obtained with the Euler-Euler approaches show significant dependency on internal model constants and that these approaches fail to predict tip vortex cavitation unless very fine grids are used.

In this paper both Euler-Euler and Euler-Lagrange approaches are briefly described. A combined model using benefits of both methods is suggested. As an example, numerical simulations of a cavitating propeller at a Reynolds number of $1.4{\cdot}10^6$ are presented. The original Euler-Lagrange approach is compared with the Euler-Euler and combined Euler-Euler/Euler-Lagrange models. The latter is seem to provide a very good compromise between accuracy and computational efficiency.

NUMERICAL MODEL

In the present work an in-house solver FreSCo$^+$, a joint development of Hamburg University of Technology (TUHH) and the Hamburgische Schiffbau-Versuchsanstalt (HSVA) [11] was used. The two-phase flow is modeled as a dynamic liquid/vapor mixture with properties defined by a supplementary vapour-volume fraction and only one set of Navier-Stokes equations is solved.

For the solution of the Navier-Stokes equations for the Eulerian liquid/vapor-mixture a segregated control-volume method based on the strong conservation form of the momentum equations is used. It employs a cell-centred, co-located storage arrangement for all transport properties. Structured and unstructured grids, based on arbitrary polyhedral cells or hanging nodes, can be used. The implicit numerical approximation is second-order accurate in space and time. Integrals are approximated using the conventional mid-point rule. The solution is iterated to convergence using a pressure-correction SIMPLE scheme. Accordingly, local density changes due to the change of vapor content have to be considered. Various turbulence-closure models are available with respect to statistical (RANS) or scale-resolving (LES, DES) approaches. Since the data structure is generally unstructured, suitable pre-conditioned iterative sparse-matrix solvers for symmetric and non-symmetric systems (e.g. GMRES, BiCG, QMR, CGS or BiCGStab) can be employed.

Governing equations

The fluid mixture of an incompressible liquid and bubbles containing vapor and homogeneous gas is described by the

Proceedings of the Eighth International Symposium on Cavitation (CAV 2012)
Edited by Claus-Dieter OHL, Evert KLASEBOER, Siew Wan OHL, Shi Wei GONG and Boo Cheong KHOO.

ISBN: 978-981-07-2826-7 :: doi:10.3850/978-981-07-2826-7_063

isothermal Navier-Stokes equations

$$\frac{\partial \rho}{\partial t} + \nabla \cdot (\rho \mathbf{u}) = 0, \quad \frac{\partial \rho \mathbf{u}}{\partial t} + (\mathbf{u} \cdot \nabla)(\rho \mathbf{u}) = -\nabla p + \nabla \cdot \boldsymbol{\tau} + \mathbf{F}. \tag{1}$$

Here $\boldsymbol{\tau}$ denotes the viscous stress tensor and $\mathbf{F}$ represents volume forces. In the present work k-ω RANS approach [15] is used for turbulence modelling.

The mixture density ρ and mixture viscosity μ are computed as a sum of partial densities and viscosities of the fluid (f) and vapor (v)

$$\rho = \alpha \rho_v + (1-\alpha)\rho_f, \quad \mu = \alpha \mu_v + (1-\alpha)\mu_f. \tag{2}$$

Here α is the vapor volume fraction defined as the ratio between the vapor volume and the total volume of a control volume $\alpha = V_v/V$.

Euler-Euler cavitation model

Within Euler-Euler approach vapour volume fraction is computed via an additional transport equation

$$\frac{\partial \alpha}{\partial t} + \nabla \cdot (\alpha \mathbf{u}) = R. \tag{3}$$

The source term R determines the mass (volume) transfer between vapor and liquid. Several different models exist to define R, which all refer to a simplified Rayleigh-Plesset equation and employ various empirical constants. In the present work the definition suggested by Sauer [12] was used

$$R = 4\pi R_b^2 n_0 \sqrt{\frac{2}{3}\frac{|p_v^* - p|}{\rho_l}}(1-\alpha) sign(p_v^* - p), \tag{4}$$

where n_0 denotes the bubble density and R_b refers to a representative local bubble radius. Note that the original vapor pressure used by Sauer is replaced by a modified pressure p_v^* to take into account turbulence influence on the cavitation inception as suggested by Singhal et al. [14]

$$p_v^* = p_v + 0.195\rho k, \tag{5}$$

with k being the turbulent kinetic energy.

The model proved to be adequate for sheet cavitation prediction in case of using adjusted internal model constants [1]. Nevertheless this approach has an intrinsic no-slip condition between the phases, doesn't allow to take into individual bubble behaviour and interaction between bubbles, doesn't consider inhomogeneous or transient water quality aspects and scale effects.

Euler-Lagrange cavitation model

The Euler-Lagrange approach allows to overcome some of the above mentioned drawbacks of the Euler-Euler approach. Within this approach individual bubbles composing discrete phase are started upstream of the cavitation region and tracked in the surrounding fluid [2, 16].

The kinematics of the bubbles is computed from a momentum equation [9, 10]

$$\frac{d\mathbf{v}}{dt} = -2\mathbf{g} + 3\frac{D\mathbf{u}}{Dt} + \frac{3}{4}\frac{C_D}{R}|\mathbf{u}-\mathbf{v}|(\mathbf{u}-\mathbf{v}) + \frac{3}{4}C_L\frac{(\mathbf{u}-\mathbf{v})\times\boldsymbol{\omega}}{\alpha} + \frac{3}{R}(\mathbf{u}-\mathbf{v})\frac{dR}{dt}, \tag{6}$$

where $\alpha = |\omega|R/|\mathbf{u}-\mathbf{v}|$, C_L is a lift coefficient, C_D is a drag coefficient as given in [10].

The solution of the modified Rayleigh-Plesset equation as published by [4] is used to determine the evolution of the bubble diameter

$$R\ddot{R} + \frac{3}{2}\dot{R}^2 = \frac{1}{\rho_f}\left[p_v + p_g - p_\infty - \frac{2\sigma}{R} - \frac{4\mu_f}{R}\dot{R}\right] + \frac{(\mathbf{u}-\mathbf{v})^2}{4}, \tag{7}$$

where p_g is the gas pressure inside the bubble defined by a polytropic compression with a polytropic exponent k=1.4, p_∞ is the local pressure outside the bubble and σ is the surface tension.

In turbulent flows it might be important to take into account bubble break-up which occurs due to turbulent fluctuations and bubble/turbulent eddy collision. The probability based model of Martinez-Bazan et al. ([7, 8]) displayed very good agreement with experiments for a bubble break-up in a fully developed turbulent flow over a wide range of bubble sizes. This model has been implemented into the current framework.

To obtain fluid parameters needed for solution of the equations (6) and (7) a gradient-based interpolation from the fluid mesh cell center to the position of the bubble (defined by the position of it's center) is performed for each bubble [16]. The vapour-volume fraction is calculated from the discrete bubbles for each fluid mesh cell via Gaussian kernel-based interpolation as suggested by Shams et al. [13].

Combined model

The main drawback of the Euler-Lagrange approach are increased computational demands due to the large number of tracked bubbles. Typically, momentum and Rayleigh-Plesset equations are solved via Crank–Nicolson scheme for several millions bubbles. Note that time step used in these scheme is about thousand times smaller than for the Euler phase due to the very small bubble sizes. An efficient hybrid MPI/OpenMP parallelization has been implemented [16] but the model is still quite expensive in terms of required time/computational resources.

To reduce the computational cost a combined Euler-Euler/Euler-Lagrange approach is suggested. Within this approach bubbles initialized only in a certain area which requires more accurate consideration (e.g. tip vortex) and Euler-Lagrange solution is used there, the rest of domain is computed via an Euler-Euler approach.

The numerical algorithm of the combined model for one Eulerian physical time step (non-parallel version) can be described as follows:

1. Update Eulerian time $t_f^{n+1} = t_f^n + \triangle t_f$
2. Calculate new mixture pressure, velocities and turbulent quantities by solving equations (1)
3. Inject specified number of nuclei at initial position. The initial nuclei spectra (nuclei concentration and initial diameter distribution) depends on a water quality and is either known from experiments or estimated. The initial position is defined by an area upstream of the cavitation region. Bubbles are started randomly within this area

4. For each of the bubbles proceed while Lagrangian time $t_{v_i} \leq t_f^{n+1}$:
   - Update Lagrangian time for ith bubble t_{v_i}=t_{v_i}+$\triangle t_{v_i}$
   - Update bubble size and position solving iteratively equations (6) and (7)
5. Using above described probability based model compute bubbles break-up
6. Calculate vapor-volume fraction from bubbles
7. Solve vapor volume fraction equation (3) imposing calculated on the previous step vapor-volume fraction from bubbles (in cells where it is greater than zero)
8. Update mixture density and viscosity

RESULTS

Test case description and numerical setup

Cavitation tests for a five-blade controllable pitch propeller (Potsdam Propeller Test Case - PPTC, `http://www.sva-potsdam.de/pptc`) were conducted in the large test section of the cavitation tunnel K15A of the SVA Potsdam for various operational points. The propeller diameter refers to D=250mm. It features a chord length at r/R=0.7 of c/D= 0.417, a pitch ratio of 1.635 at r/R=0.7, a hub-diameter ratio of 0.3, an area ratio of 0.779 and a skew angle of 18.8°. The operating conditions for the selected case refer to an advance coefficient of 1.01, a cavitation number of 1.96, Reynolds number at r/R=0.7 of $1.4 \cdot 10^6$ and air content of 80% of saturation.

For numerical simulations two computational grids has been generated - one has $4 \cdot 10^6$ cells with refinement for one blade in order to assess the blade resolution dependency (Figure 1). Another grid has $12 \cdot 10^6$ cells with additionally refined region in tip vortex (Figure 2). It has been generated accordingly to the authors' previous experience that Euler-Euler models requiring very fine grid resolution in the tip vortex region [17].

A uniform velocity of 5.301 m/s was imposed at the inflow boundary. At the outlet boundary a uniform pressure was specified providing desired cavitation number. No-slip walls with wall functions were assigned to the hub and propeller blades. A slip-wall boundary condition was employed along the outer circumference.

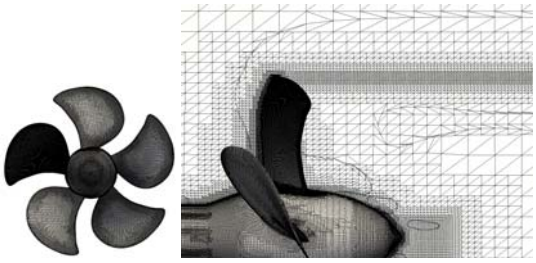

Figure 1: PPTC propeller, (left) blades surface mesh, (right) XY plane view

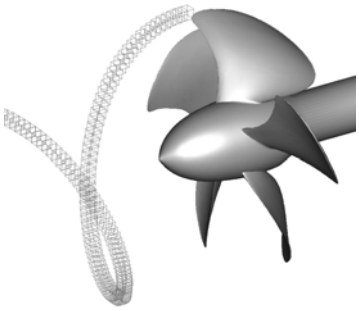

Figure 2: Refined vortex region (contains $\sim 8 \cdot 10^6$ cells)

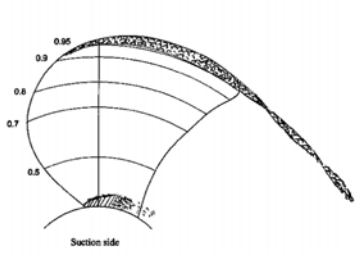

Figure 3: PPTC propeller, experimental cavitation pattern

The investigated cavitation case reveals tip vortex and suction side cavitation in the near-hub region. Figure 3 shows a sketch of the cavitation pattern observed in experiments with high-speed video [3].

Euler-Euler model results

Figure 4 shows isosurface of vapor volume fraction equal to 0.2 obtained on the $4 \cdot 10^6$ cells grid by the Sauer Euler-Euler model. As expected, sheet cavitation on the blade suction side and hub vortex cavitation are predicted quite well, but no cavitation is observed in the tip vortex cavitation. The resolved vortex is not strong enough to cause the required pressure reduction in it's core which is the only mechanism in the Euler-Euler approach responsible for the the cavitation inception. Similar results were obtained with use of other Euler-Euler models [1].

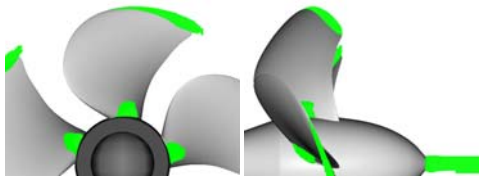

Figure 4: PPTC propeller, Euler-Euler model results, $4 \cdot 10^6$ cells grid

With grid refinement in the tip vortex region, computed pressure drops enough to start cavitation. As one can see on Figure 5 cavitation pattern is now reproduced quite successfully. It required about eight million additional nodes to resolve tip vortex correctly with a current model. Less dissipative turbulence models like LES/DES or special techniques aimed at reduction of turbulent viscosity in the vortex region i.e.

vorticity confinement methods [5] might reduce such severe requirements to the grid quality. That is the subject of further studies.

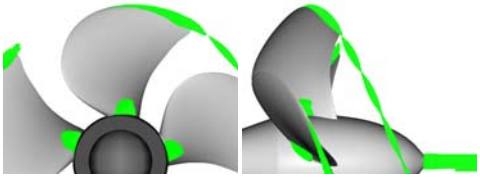

Figure 5: PPTC propeller, Euler-Euler model results, $12 \cdot 10^6$ cells grid

Euler-Lagrange model results

Nuclei distribution required for the Euler-Lagrange model has been measured experimentally with the Laser Doppler Anemometry (LDA) technique under the aegis of the BMWi-project *KonKav-I*. Experimental work was performed by the Institute for General Electrical Engineering of the University of Rostock. Figure 6 displays measured bubble spectra for the considered test case. Measured bubble diameters lay within range of 10 to 200 microns with most of bubbles within 20-120 microns range.

At every Eulerian physical time 140 bubbles were injected in the area upstream the propeller at radius of tip blade as shown in Figure 6. Number of injected bubbles corresponds to the number of nuclei measured in the experiment and their radius is randomly chosen according to the measured probability density function. Bubbles injected in this area develop farther downstream and get into the tip vortex region of one of the blades. Note that bubble injection area is restricted to one blade tip area and doesn't cover the whole domain which otherwise would require much more injected bubbles.

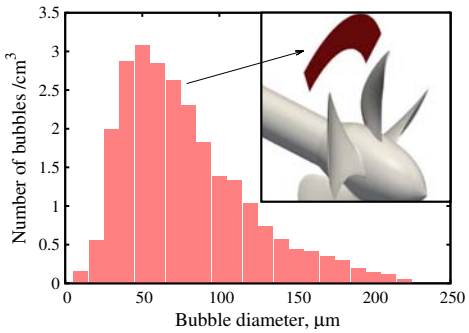

Figure 6: PPTC propeller, nuclei distribution at $\sigma = 1.96$ and air content 80% used to release bubbles in the selected area upstream the propeller blades

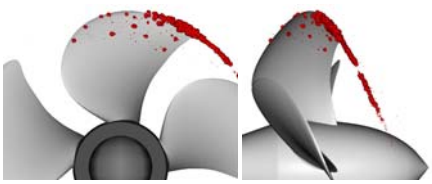

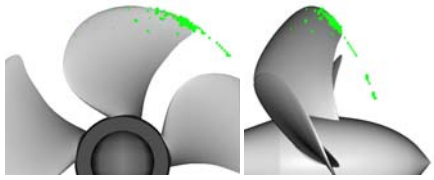

Figure 7: PPTC propeller, Euler-Lagrange model, coarse grid. Vapor bubbles (top), vapor volume fraction (bottom)

Figure 7 displays instantaneous snapshot of vapor bubbles and corresponding vapor volume fraction computed from these bubbles on $4 \cdot 10^6$ cells grid. In contradistinction to the similar Euler-Euler model results (Figure 4), Euler-Lagrange model predicts tip vortex cavitation even with this grid, but cavitating vortex weakens and dissapears downstream the blade quite rapidly. Vapor bubles grow in the low pressure region at the blade tip and convected farther downstream, but then they are condensing due to the too high pressure given by the Euler phase solution on relatively coarse grid. Single travelling vapor bubbles are also found near the upper part of the blade. They cannot be predicted by the Euler-Euler approach because of the no-slip condition between phases and relatively high pressure in this region, but within the Euler-Lagrange approach, which considers bubble movement separately, single bubble may penetrate higher pressure regions and "survive" there some time. No cavitation can be seen in the near-hub region as no bubbles were injected there.

Same as for Euler-Euler simulations, with refined grid tip vortex core pressure reduces and vapor bubbles now not condense but develop in the tip vortex. Cavitation pattern predicted by the Euler-Lagrange model (Figure 8) is in a fair agreement with the experiment as well as with the Euler-Euler model results.

It should be also mentioned, that in spite of the similarity for the cavitation pattern computed by two approaches, Euler-Lagrange model has much more potential benefits arising from the discrete model for the vapor phase, which better corresponds to the physics of the cavitation phenomenon. Among them are erosion prediction, which requires to account of impact pressure from individual bubbles near the wall, acoustic pressure calculations, which also require individual bubble information, water quality and scale effects, which are not considered by the Euler-Euler approach, but may be addressed by the Euler-Lagrange method [6].

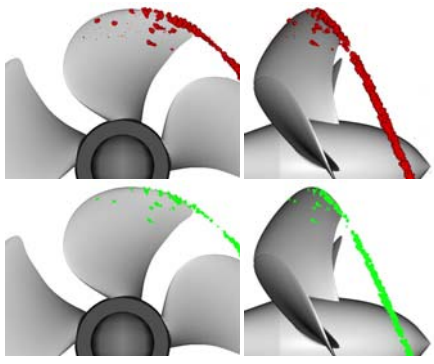

Figure 8: PPTC propeller, Euler-Lagrange model, refined grid. Vapor bubbles (top), vapor volume fraction (bottom)

Combined model results

As discussed above, a combination of the Euler-Euler and Euler-Lagrange approaches has most of the benefits of the Euler-Lagrange model in specific regions of interest and reduced computational costs due to use of simplified Euler-Euler approach in the rest of the domain. Figure 9 shows results obtained with the combined model with the refined grid of $12 \cdot 10^6$ cells. As expected, cavitating tip vortex is predicted very similar to the Euler-Lagrange model results (compare with Figure 8) when near-hub cavitation is predicted similar to Euler-Euler approach (compare with Figure 5).

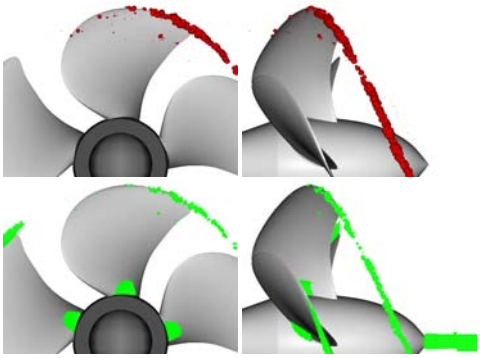

Figure 9: PPTC propeller, combined Euler-Euler/Euler-Lagrange model, refined grid. Vapor bubbles (top), vapor volume fraction (bottom)

Table 1 analyses computational times required to simulate one propeller revolution (360 time steps) with different models. All simulations has been performed with the $12 \cdot 10^6$ cells grid on the North-German Supercomputing Alliance (HLRN-II) supercomputing system ICE2 (`www.hlrn.de`) with 128 Intel Xeon Gainestown CPU cores. Euler-Euler simulations required 5.2 wall-clock hours to simulate one revolution. Same simulations with Euler-Lagrange model restricted to the tip vortex region required 30% more computational time. Estimated computational time for simulations of the whole domain with Euler-Lagrange model is at least five time more as there would be five times more injected bubbles. Therefore, combined Euler-Euler/Euler-Lagrange model which required only 35% more time as compared to the Euler-Euler model does significantly reduces computational efforts.

Table 1: Computational time for one propeller revolution

Model	Time
Euler-Euler	5.2 hours
Euler-Lagrange (tip vortex only)	6.7 hours
Euler-Lagrange (whole domain)	est. 23.3 hours
Combined Euler-Euler/Euler-Lagrange	7 hours

CONCLUSIONS

Three approaches to cavitation modelling has been described - the traditional Euler-Euler approach based on solution of an additional transport equation for vapor volume fraction, the advanced Euler-Lagrange approach considering vapor phase as a discrete phase composed of numerous vapor bubbles and the combination of these two approaches. The latter aimed to use benefits of both models - fair prediction accuracy of the Euler-Lagrange approach and reduced computational costs of the Euler-Euler approach.

Numerical results for a cavitating propeller flow computed with all three models were presented and compared with the experiments. The Euler-Euler model failed to predict the tip vortex cavitation unless using very fine grids in this region. Euler-Lagrange model seems to be less demanding to grid size but still require reliable prediction of the pressure and velocity fields. The combined model results are very close to the results of the Euler-Lagrange model in the tip vortex and Euler-Euler model in the rest of the domain. At the same the combined model requires for this test case about three times less computational time as compared to the pure Euler-Lagrange model.

The present techniques can be applied to a wide range of multiphase engineering applications. The potential capabilities of these techniques include acoustic pressure calculation and erosion risk estimation, study of water quality and scale effects. These are the topics of the current and future work.

ACKNOWLEDGMENTS

The current work is a part of the research project funded by German Ministry of Economics and Technology (BMWi; Grant Nr. 3SX286A) in the framework of the ”Schifffahrt und Meerestechnik für das 21. Jahrhundert” research initiative. The experimental data were obtained by our colleagues from the University of Rostock. The simulations were performed on the HLRN-II supercomputer system at the North German Cooperation for High-Performance computing (HLRN). This support is gratefully acknowledged by the authors.

REFERENCES

[1] smp’11 workshop on cavitation and propeller performance. In International Symposium on Marine Propulsors, Hamburg, Germany, 2011.

[2] M. Abdel-Maksoud, D. Hänel, and U. Lantermann. Modeling and computation of cavitation in vortical flow. International Journal of Heat and Fluid Flow, 31(6):1065 – 1074, 2010.

[3] H.-J. Heinke. Potsdam propeller test case (PPTC). Measurement of the propeller characteristics and cavitation tests with the model propeller VP1304 at different gas contents of the tunnel water. Technical report 3890.1, SVA Potsdam Model Basin, Potsdam, 2012.

[4] C.-T. Hsiao and G. Chahine. Prediction of tip vortex cavitation inception using coupled spherical and nonspherical bubble models and Navier–Stokes computations. J. Marine Sci. Technol., 8:99–108, 2004.

[5] M. Manzke and T. Rung. Propeller flow predictions using turbulent vorticity confinement. In Proceedings of the V European Conference on Computational Fluid Dynamics ECCOMAS CFD 2010, Lisbon, Portugal, 2010.

[6] T. Maquil, M. Abdel-Maksoud, B. Cankurt, T. Rung, P. Schiller, and S. Yakubov. Simulation of water-quality effects for cavitating engineering flows. In CD-ROM

proceedings of the WIMRC 3rd International Cavitation Forum, Warwick, 2011.

[7] C. Martinez-Bazan, J. Montanes, and J. C. Lasheras. On the breakup of an air bubble injected into a fully developed turbulent flow. Part 1. Breakup frequency. J. Fluid Mech., 401:157–182, 1999.

[8] C. Martinez-Bazan, J. Montanes, and J. C. Lasheras. On the breakup of an air bubble injected into a fully developed turbulent flow. Part 2. Size PDF of the resulting daughter bubbles. J. Fluid Mech., 401:183–207, 1999.

[9] M. R. Maxey and J. R. Riley. Equation of motion for a small rigid sphere in a nonuniform flow. Journal Physics of Fluids, 26(4):883–889, 1983.

[10] G. Oweis. Capture and inception of bubbles near line vortices. Journal Physics of Fluids, 17:022105, 2005.

[11] T. Rung, K. Wöckner, M. Manzke, J. Brunswig, C. Ulrich, and A. Stück. Challenges and Perspectives for Maritime CFD Applications. Jahrbuch der Schiffbautechnischen Gesellschaft, 103, 2009.

[12] J. Sauer. Instationär kavitierende Strömungen—Ein neues Model, basierend auf Front Capturing (VoF) und Blasendynamik. PhD thesis, Universität Karlsruhe, 2000.

[13] E. Shams, J. Finn, and S. Apte. A numerical scheme for Euler-Lagrange simulation of bubble flows in complex systems. International Journal for Numerical Methods in Fluids, 66, 2010.

[14] A. Singhal, M. Athavale, H. Li, and Y. Jiang. Mathematical basis and validation of the full cavitation model. J. Fluids Eng., 124(3):617–624, 2002.

[15] D. Wilcox. Turbulence Modeling for CFD. DCW Industries, Inc., 2 edition, 2004.

[16] S. Yakubov, B. Cankurt, M. Abdel-Maksoud, and T. Rung. Hybrid MPI/OpenMP parallelization of an Euler-Lagrange approach to cavitation modelling. Computers and Fluids, 2012. Doi:10.1016/j.compfluid.2012.01.020.

[17] S. Yakubov, B. Cankurt, T. Maquil, P. Schiller, M. Abdel-Maksoud, and T. Rung. Cavitation simulations of the Potsdam propeller test case. In Proceedings of the Workshop on Cavitation and Propeller Performance. Second International Symposium on Marine Propulsors - SMP'11, pages 84–92, Hamburg, Germany, 2011.